ZESZYTY NAUKOWE POLITECHNIKI RZESZOWSKIEJ **Nr 284**
Mechanika z. 84 (3/12) **2012**

Tomasz TRZEPIECIŃSKI
Rzeszow University of Technology

NUMERICAL MODELING OF THE DRAWBEAD SIMULATOR TEST

The work contains the results of experimental researches and numerical simulations of friction test that simulate the friction conditions in drawbead during sheet metal forming. The numerical model of the drawbead friction simulator test has been created using MSC.Marc + Mentat 2010. Simulations have been performed to determine a stress state in pulled sample during the drawbead simulator test. The isotropic and two anisotropic Hill (1948) and Barlat (1991) material models were used in simulations taking into consideration sample orientation according to the rolling direction of the sheet. The samples for friction tests were cut along and transverse to the rolling direction of the sheet. It was found that the yield criterion has a strong influence on the distribution and the value of normal and shear stresses in the sample. Furthermore, the values of analyzed stresses were changed in the sample width.

Keywords: coefficient of friction, drawbead, FEM, friction, numerical modeling, sheet metal forming

1. Introduction

In the deep drawing process a few regions exist, i.e. the wall, bottom and flange of the cup, with different stress state, strain state, sliding speed and friction conditions. In this regard, a series of tribological tests modeling friction conditions in different parts of the drawpiece were elaborated. Many friction tests were developed to modeling of friction conditions in specified regions of formed part. To model the friction in the drawbead regions of the drawpiece the drawbead simulators (DBS) are used based on conception of Nine [1]. Drawbeads generate a stable tensile force opposite to the sheet drawing direction by introducing a series of local bending, straightening and reverse bending deformation on the sheet (Fig. 1) [2]. Resistance to friction occurred on the contact surface brakes free metal flow as a result of that in deformed metal we can distinguish zones with different deformation extent. To negative results of friction affecting in the deep drawing process belong i.e. increasing non-uniformity of deformation, increasing loading force and worsening quality of the drawpiece

surface. Furthermore, existing of the drawbead strongly influences on the springback phenomenon of the drawpiece after removing from dies [3, 4].

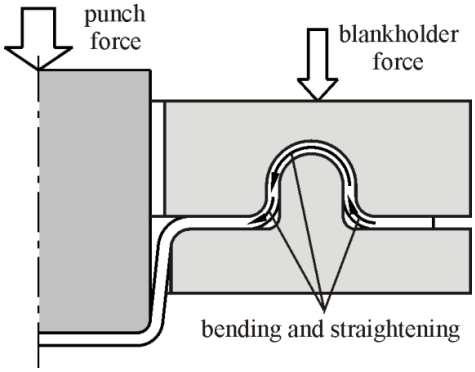

Fig. 1. Deformation of the sheet in the drawbead region

General application of numerical simulations of the sheet metal forming for proper functioning inquires the knowledge of a suitable mathematical description of friction behaviour. Hence, better understanding of friction role and reliable methods for quantitative values of the friction coefficient determination is necessary. In spite of developing of numerical methods [5] calculation of friction coefficient value, the role of experimental methods of the friction coefficient value is still essential. The experimental results based on drawbead simulator [6] indicate that the dominant factors in determining both restraint force and blank thinning are bead penetration and material type (particularly the flow stress and strain hardening exponent).

2. Materials and methods

In the experimental researches an aluminium alloy AA5251 H14 with thickness 1mm was used. The nominal gauge thickness was 1.00 mm whereas the average sheet thickness was 1.00+–0.01 mm based on measurements taken at several locations. A tensile test in the universal testing machine was carried out to determine mechanical properties of the sheets along the rolling direction: yield stress σ, ultimate strength σ_m, elongation A_{50}, anisotropy coefficient r, strain hardening coefficient K and strain hardening exponent n (Table 1). The samples for tensile tests were cut in both directions: along the rolling direction (0^o), transverse to the rolling direction (90^o) and by 45^o angle from rolling direction.

The value of the tensile parameters (Table 1) has been averaged according to:

$$x_{\text{mean}} = \frac{(x_0 + 2x_{45} + x_{90})}{4} \tag{1}$$

where x is a tensile parameter and the subscripts refer to the specimen orientation.

Surface roughness parameters measurements were carried out using the Alicona Infinite Focus instrument to determine the main 3D roughness parameters (Table 2): the roughness average *Sa*, the root mean square roughness parameter *Sq*, the highest peak of the surface *Sp*, the maximum pit depth *Sv*, the surface skewness *Ssk*, the surface kurtosis *Sku*, the 10-point peak-valley surface roughness *Sz*, the density of summits *Sds*, the texture aspect ratio of the surface *Str*, the surface bearing index *Sbi*, the core fluid retention index *Sci*, the valley fluid retention index *Svi*.

Table 1. The mechanical properties of the AA5251 H14 sheet

Orientation	**Mechanical properties**					
	$R_{p0,2}$ **[MPa]**	R_m **[MPa]**	A_{50}	C **[MPa]**	n	r
0^o	212	234	0.04	254	0.058	0.478
45^o	203	231	0.04	242	0.062	0.689
90^o	210	241	0.04	227	0.078	0.786
Average	208	234.25	0.04	241.25	0.065	0.6605

Table 2. The surface roughness parameters of the AA5251 H14 sheet

Sa **[µm]**	***Sq*** **[µm]**	***Sp*** **[µm]**	***Sv*** **[µm]**	***Ssk***	***Sku***	***Sz*** **[µm]**	***Sds*** **[Peaks/mm^2]**	***Str***	***Sbi***	***Sci***	***Svi***
0.340	0.423	2.48	1.62	0.298	3.34	3.3	697	0.036	0.243	1.67	0.094

In the drawbead simulator the sheet metal is pulled to flow between three cylindrical rolls of equal radii 20 mm (Fig. 2) [7]. The specimens were cut along and transverse to the rolling direction into 200 mm length and 20 mm width strips.

To realize lubrication conditions machine oil L-AN 46 was used. Lubricant was applied in excess to the test strips so that film thickness was determined by the process. The roughness average Ra parameter measured along generating line of rolls was equal 1.25 µm. The rolls were made of cold-work tool steel X165CrV12.

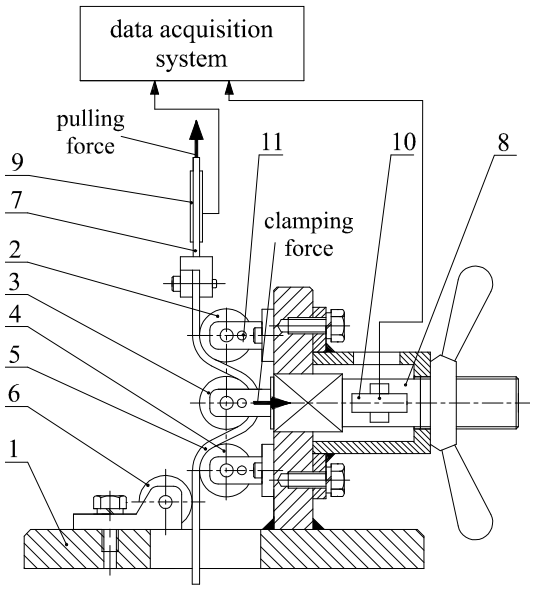

Fig. 2. Measurement system used for friction testing: 1 – frame, 2 – front roll, 3 – middle roll, 4 – back roll, 5 – specimen, 6 – supporting roll, 7 and 8 – tension members, 9 and 10 – extensometers, 11 – fixing pin

The very high wrap angle of the middle roll produces a very high slide resistance and may be resulted on over-increasing plastic tension of the sheet and fracture. The main purpose of this clearance is to prevent locking of the sheet between the rolls, especially during the test realized with fixed rolls. The clearance c (Fig. 3) between working rolls equal 2.34 mm was maintained. Further, the tests were carried out for middle roll penetration p (Fig. 3) equals 18 mm. The total wrap angle around all rolls at full middle roll penetration was equal about 244.18°.

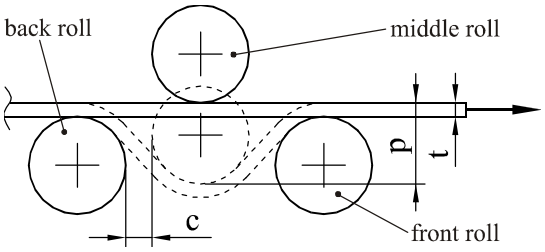

Fig. 3. Geometrical parameters of drawbead simulator test

The restraining force consists of a frictional portion and a bending portion. So, to determine the friction coefficient two tests must be carried out. In first test the specimen is pulled between cylindrical rolls free rotatable about their axis. Then the pulling force (denoted as D_{roll}) and clamping force (C_{roll}) measure the bending and unbending resistance of the sheet under “frictionless” conditions.

The sheet is displaced between rotatable rolls so the friction between the sheet and rolls is minimized. In second test the specimen is pulled between fixed rolls. Friction opposes the sliding of the sheet over the fixed tolls. The pulling D_{fix} and clamping C_{fix} forces measure the combined loads required to slide and to bend and unbend the sheet. During both tests the supporting roll was free to rotate about its axis. The pulling and clamping forces were measured using load cells. The strip was drawn as a distance of 40 mm. The sliding speed was set to 1 mm/s. The drawing distance is chosen to be long enough such that a plateau is reached when evaluating the thickness changes and stress history for an element passing through the drawbead.

It was found [8] that the angle of wrap that corresponds to the actual engagement of the strip with the roller or bead was not taken into account in the derivation by Nine [1]. As penetration increased, the wrap angle increased. However, it was not until very deep penetration that the tangent-to-tangent bead wrap assumption became approximately valid [9].

When the wrap angle is not equal 180° the friction coefficient has been calculated from following equation [10]:

$$\mu = \frac{D_{fix} - D_{roll}}{C_{fix}} \cdot \frac{\sin\Theta}{2\Theta} \tag{2}$$

where Θ is the quarter contact angle of actual engagement of the strip over the bead.

The values of all force values were constantly recorded using electric resistance strain gauge technique, 2-channel universal amplifier of data acquisition system and computer PC.

3. Numerical modeling

The simulation of the drawbead simulator test was conducted using MSC.Marc + MENTAT 2010 program. The rolls were defined as rigid surfaces and suitable boundary conditions corresponding to experimental conditions. The geometric model of the blank consists of 3600 quad4 shell elements [11] with a size of 0.5 x 0.5 mm and 5 integration points through the shell thickness which are necessary for an acceptable solution [12, 13]. Initially the middle roll is moved down through a distance 18 mm to bend the sheet metal while the leading end of the sheet metal is fixed (Fig. 4a). Displacement was then applied to one end of the sample after the required wrap angle was obtained (Fig. 4b). The sample was drawn a distance of 40 mm.

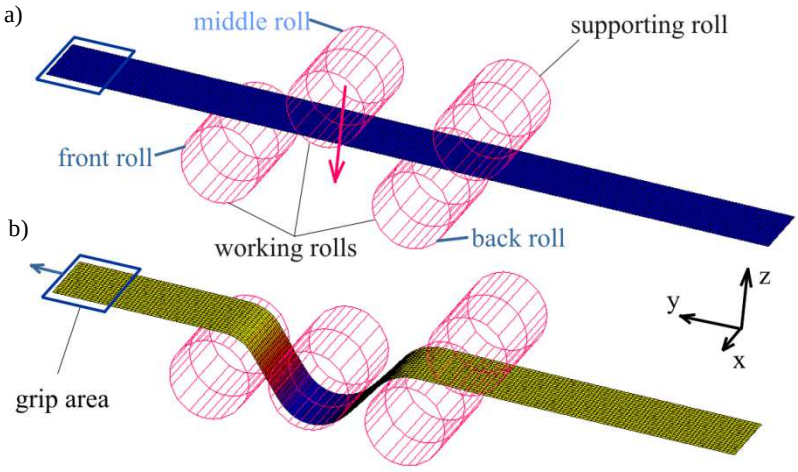

Fig. 4. Geometry of FEM model of drawbead simulator test: a) initial configuration, b) start of drawing stage

An elasto-plastic material model approach was implemented. Three material models have been simulated. In first model the plastic behavior of the sheet material was described by the von Mises yield criterion [14]. In the second model the anisotropy of material has been established using Hill (1948) yield criterion [15] which may be applied for material description of aluminium alloys [16]. In third model the Barlat (1991) [17] yield criterion has been applied. In case of anisotropy material models both 0° and 90° sample orientations have been examined. The elastic behaviour is specified in numerical simulations by the value of Young's modulus, E = 70000 MPa, and of Poisson's ratio v = 0.33. The mass density of sheet metal is set to 2690 kg·m^{-3}. The isotropic hardening behaviour implemented in FEM model uses the Hollomon power-type law. The parameters C and n in Hollomon equation have been fitted on stress-strain curve of the tensile test and have been written in Table 1.

To describe contact conditions the Coulomb friction law was applied Eq:

$$f_t = \mu f_n \frac{2}{\pi} \arctan\left(\frac{\|v_r\|}{\text{RVCNST}}\right) T \tag{3}$$

where: f_t – tangential (friction) force,
μ – friction coefficient,
f_n – normal force,
$\|v_r\|$ – relative sliding velocity,
RVCNST – value of the relative velocity below which sticking occurs,
T – tangential vector in the direction of the relative velocity.

The value of RVCNST factor was ass umed as 1% typical relative sliding velocity $\|v_r\|$ [18]. Two numerical models have been examined. In the first numerical model, the friction coefficient equals to zero was assumed which correspond to free rotating rolls. In the second model, the value of the friction coefficient was complied with experimental results (Fig. 5).

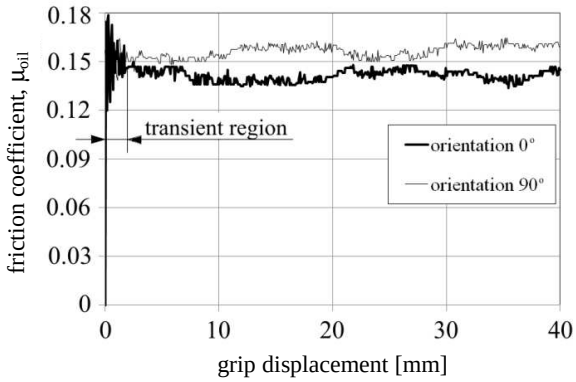

Fig. 5. Friction coefficient μ_{oil} versus grip displacement

The distributions of effective strain for different yield criteria in the moment of full penetration have considerably differed from each other (Fig. 6). Maximal values of effective strains for Hill yield criterion for sample oriented 0° according to the rolling direction of the sheet are higher of about 0.006 than for sample cut transverse to the rolling direction of the sheet. Similar relationship exists for Barlat's material model. Furthermore, the points of occurrence of maximal effective strains depend on assumed material model. The distribution of effective strain on the sample width in the place of contact of middle roll with the sample was non uniform on the sample width. This effect cannot be determined assuming plane strain conditions in 2D simulations of sheet bending.

The distribution of normal stress and shear stress in transverse section after drawing distance 20 mm were shown in Fig. 7, respectively. The maximal values of normal stress and shear for all material yield criteria are on the edge of the sample. The values of stresses for Barlat's material model regarding both orientations are the most closest to the isotropic model. The local minimum at the middle of A-A' section is connected with deformation of the sheets during bending over the middle roll. It causes that the sheet contacts locally with the bead and friction force are not constant on the sample width. In case of both Hill 0° and Hill 90° yield models the distribution of normal and shear stresses on the width of the sample are more uniform. The distribution of stresses for both

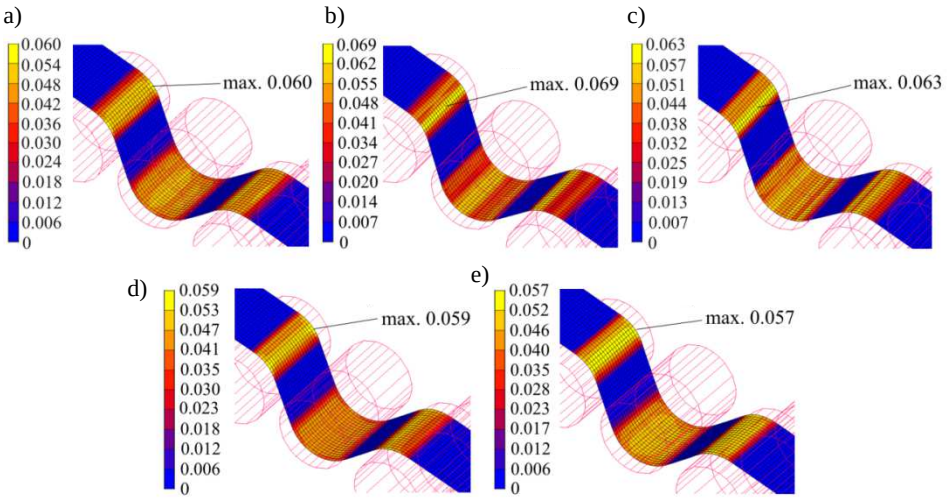

Fig. 6. The distribution of effective strain for analyzed material models: a) isotropic, b) Hill 0^o, c) Hill 90^o, d) Barlat 0^o, e) Barlat 90^o

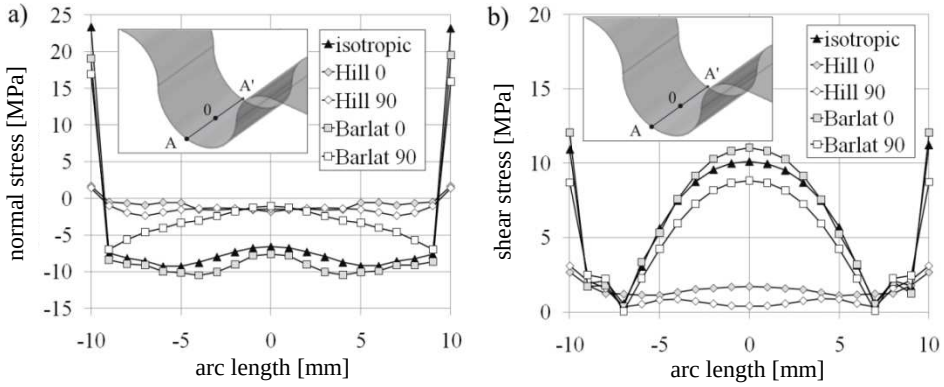

Fig. 7. The distribution of normal stress (a) and shear stress (b) along A-A' section

analyzed orientations is similar but the sample orientation effects on the value of stresses. The values of shear stresses for Hill's yield criterion have considerably lower values than others models and were more uniform especially in the middle part of the analyzed width of sample.

4. Conclusions

Two main problems were studied in this article: experimental researches of frictional conditions of AA5251 H14 aluminium alloy using drawbead simulator test proposed by Nine [9], and numerical simulations after mentioned friction test. The material model has been described by isotropic and anisotropic yield criteria. The main results of our research are as follows:

1. Sample orientation has clear effect on the value of the friction coefficient. In case of sample orientation 90^o the higher value of friction coefficient than in case of sample orientation 0^o was determined.
2. The yield criterion has a strong influence on the distribution of normal and shear stress. But results of stress distribution for both 0° and 90° orientations of strips are quite similar.
3. As it has been found the values of normal and shear stress on the width of the sheet are changed. It has been concluded that in order to obtain representative results of numerical simulations of Nine friction test, conducting simulation of a 3D model of the drawbead is necessary.

References

[1] Nine H.D.: Draw bead forces in sheet metal forming. Proc. Symp. Mechanics of Sheet Metal Forming: Behaviour and Deformation Analysis, Warren, Plenum Press, Michigan 1978, 179-211.
[2] Meinders T.: Developments in numerical simulations of the real-life deep drawing process, doctoral thesis, University of Twente-Enschede, 2000.
[3] Taherizadeh A., Ghaei A., Green D.G., Altenhof W.J.: Finite element simulation of springback for a channel draw process with drawbead using different hardening models, Int. J. Mech. Sci., 51 (2009), 314-325.
[4] Gan W., Wagoner R.H.: Die design method for sheet springback, Int. J. Mech. Sci., 46 (2004), 1097-113.
[5] Stachowicz F., Trzepieciński T.: ANN application for determination of frictional characteristics of brass sheet metal, J. Artif. Intell., 1 (2004), 81-90.
[6] Livatyali H., Firat M., Gurler B., Ozsoy M.: An experimental analysis of drawing characteristics of a dual-phase steel through a round drawbead, Materials & Design, 31 (2010), 1639-1643.
[7] Trzepieciński T.: Badania oporów tarcia wywołanych działaniem progów ciągowych w procesie kształtowania blach, Rudy Metale Nieżelazne, 55 (2010), 345-349.
[8] Manjula N.K.B., Nanayakkara P., Hodgson P.D.: Determination of drawbead contacts with variable bead penetration, Comp. Methods Mat. Sci., 6 (2006), 188-194.
[9] Green D.E.: An experimental technique to determine the behavior of sheet metal in a drawbead, SAE Technical Paper Series, 2001- 01-1136.

[10] Nanayakkara N.K.B.M.P., Kelly G.L., Hodgson P.D.: Determination of the coefficient of friction in partially penetrated draw beads, Steel GRIPS, 2, Suppl. Metal Forming, 2004, 667-682.
[11] MSC.Marc Volume B: Element Library Version 2010, MSC.Software Corporation, 2010.
[12] Larsson M.: Computational characterization of drawbeads A basic modeling method for data generation, J. Mat. Proc. Technol., 209 (2009), 376-386.
[13] Trzepieciński T., Gelgele H.L.: Investigation of anisotropy problems in sheet metal forming using finite element method, Int. J. Mat. Form., 4 (2011), 357-359.
[14] Von-Mises R.: Mechanik der festen Körper im plastisch deformablen Zustand, Nachr. Ges. Wiss. Göttingen, 1913, 582.
[15] Hill R.: A theory of the yielding and plastic flow of anisotropic metals, Proc. of the Royal Society of London, A 193 (1948), 281-297.
[16] Yoon J.W., Barlat F., Chung K., Pourboghrat F., Yang D.Y.: Earing predictions based on asymmetric nonquadratic yield function, Int. J. Plasticity, 16 (2000), 1075-1104.
[17] Barlat F., Lege D.J., Brem J.C.: A six-component yield function for anisotropic metals, Int. J. Plasticity, 7 (1991), 693-712.
[18] MSC.Marc Volume A: Theory and user information. Version 2010, MSC.Software Corporation, 2010.

MODELOWANIE NUMERYCZNE TESTU SYMULATORA PROGU CIĄGOWEGO

Streszczenie

Artykuł zawiera wyniki badań eksperymentalnych i symulacji numerycznych testu symulującego warunki tarcia na progu ciągowym podczas kształtowania blach. Model numeryczny symulatora progu ciągowego został utworzony za pomocą programu MSC.Marc + Mentat 2010. Symulacje zostały wykonane, aby określić stan naprężeń w przeciąganej próbce podczas próby tarcia. W symulacjach zaimplementowano model izotropowy właściwości mechanicznych blachy oraz dwa modele anizotropowe Hilla (1948) oraz Barlata (1991), a także uwzględniono orientację próbki kierunku walcowania. Próbki do testów tarcia zostały wycięte wzdłuż oraz w poprzek kierunku walcowania blachy. Stwierdzono, że kryterium plastyczności ma istotny wpływ na rozkład i wartość naprężeń normalnych oraz ścinających w próbce. Ponadto wartość analizowanych naprężeń zmieniała się na szerokości próbki.

Słowa kluczowe: współczynnik tarcia, próg ciągowy, MES, tarcie, modelowanie numeryczne, kształtowanie blach

DOI: 10.7862/rm.2012. 6